




## Article

# The Origin and Evolution of Ore-Bearing Rocks in the Loypishnun Deposit (Monchetundra Massif, NE Fennoscandian Shield): Isotope Nd-Sr and REE Geochemical Data

Evgeniy Kunakkuzin , Elena Borisenko, Luydmila Nerovich, Pavel Serov , Tamara Bayanova and Dmitry Elizarov 

Geological Institute of Kola Science Center of Russian Academy of Sciences, 184209 Apatity, Russia; elena.s.borisenko@gmail.com (E.B.); nerovich@geoksc.apatity.ru (L.N.); serov@geoksc.apatity.ru (P.S.); tamara@geoksc.apatity.ru (T.B.); elizarov@geoksc.apatity.ru (D.E.)

\* Correspondence: kunakkuzin@geoksc.apatity.ru

Received: 28 January 2020; Accepted: 19 March 2020; Published: 21 March 2020



**Abstract:** The Monchetundra massif is located in the north-eastern Fennoscandian Shield and refers to Paleoproterozoic massifs of the East-Scandinavian Large Igneous Province. The general section of the massif comprises two parts, the lower norite-orthopyroxenite and the upper mafic zones. The lower zone is of great interest due to its associated industrial platinum group elements (PGE) mineralization. The structure and peculiar features of rocks in the lower zone were studied using a drill core from the borehole MT-70 in the south-eastern slope of the Monchetundra massif intersecting the ore zone 1 of the Loypishnun deposit (according to the CJSC Terskaya Mining Company data). A comparison of the barren and ore-bearing varieties of norites and pyroxenites in the Loypishnun deposit shows that the ore samples have the lowest negative  $\epsilon\text{Nd}$  values, a relatively more differentiated distribution spectrum with the Light rare earth elements (LREE) dominating over the Heavy REE (HREE),  $\text{Eu}/\text{Eu}^* \geq 1$ , and a higher mean content of alkali and large-ion lithophile elements (Ba, Rb, and Cs). New geochemical data indicated an origin of magmas for rocks from a layered series in the Loypishnun deposit by a high degree of melting of a LREE-rich source with a low mean content of REE. Negative  $\epsilon\text{Nd}$  values, low ISr values, and a marked negative Nb indicate that the crustal material affected the evolution of rocks in the lower zone of the massif more than in the upper zone. The formation of ore bodies in the Loypishnun deposit was governed by the crust-mantle interaction, magmatic differentiation, and association with the most differentiated varieties, and by further concentration of the ore at the late and post-magmatic stages in a highly permeable environment for fluids in the Monchetundra fault zone.

**Keywords:** Fennoscandian Shield; Paleoproterozoic intrusions; layered intrusions; Nd-Sr isotope geochemistry; contamination

## 1. Introduction

Paleoproterozoic mafic-ultramafic massifs in the Fennoscandian Shield have been long considered promising for the platinum group elements (PGE), Cu-Ni and Cr-Ti-V, mineralization. The best-known deposits and ore occurrences confined to the Fedorovo-Panskiy massif, Monchepluton, Mt. General'skaya in the Kola region, several massifs in Karelia (Olanga intrusion group), and Finland (Portimo, Penikat, Kemi, etc.). The evolution of these massifs is associated with intense magmatic activity in the early Proterozoic, which allowed them to integrate into the East-Scandinavian Large Igneous Province [1,2]. Geochronological (U-Pb, Sm-Nd, Rb-Sr, and Re-Os), isotope-geochemical

and geochemical (Rare Earth Elements (REE), Nd-Sr-He,  $\gamma$ Os) data [1–4] indicated that these massifs were subject to intense mantle plume activity. Nevertheless, the primary composition and mode of occurrence of the mantle source is still debated. Paleoproterozoic mafic-ultramafic intrusions are similar in a general geological section and occur as a differentiated rock series. However, as shown by the Monchetundra massif, mafic rocks are geochemically heterogeneous and formed at different times, which indicates a more complicated pattern of the massif evolution [5–8]. The aim of this study was to define peculiar features of rock formation in the Loypishnun PGE deposit on the basis of the Nd-Sr isotope and the geochemical data.

## 2. Geological Settings

The Monchetundra massif occurs in the north-eastern Fennoscandian Shield as the south-eastern part of the Main Ridge and the Monchegorsk ore area [3]. The intrusion is located at the junction of the Central Kola and Belomorian (White Sea) Blocks as a fragment of the Imandra-Varzuga Paleorift [9]. The general section of the massif can be divided into two parts [2,5,10]. The lower zone is mainly composed of alternating norites and orthopyroxenites; the upper zone hosts gabbroids. Rocks in the upper part have various ages and complicated interrelations. Four main rock groups can be detected in it, based on the interpretation of the geological and isotope U-Pb age data: metagabbro (2521–2516 Ma [5,6,11]), trachytoid gabbro-norites (2507–2501 Ma [3,5,7]), massive gabbro-norites (2476–2471 Ma [5,7,12]) and gabbro-pegmatites (2456–2453 Ma [5,6,11,12]). Additionally, there are later veins of gabbro-pegmatites (2445 Ma [6]) and aplites (1900 Ma [6]). Noteworthy, the occurrence of metagabbroids (2521–2516 Ma) in the upper part of the section seems to be linked to the tectonic processes. They are sometimes identified as “an early gabbroic series” [6].

The upper mafic part of the section is well-exposed; while outcrops of the lower zone are rare. The lower part of the Monchetundra massif was studied in detail during the prospecting for noble mineralization in the south-eastern part and at drilling of deep structural boreholes (M1, 765, etc., Figure 1). The lower norite-pyroxenite zone is represented by alternating orthopyroxenites, norites, and harzburgites. This zone is ~250 m thick in the south-east of the massif. The contacts between the rocks are gradational, with no sharp boundaries. However, near a contact with the Monchepluton, these rocks produce irregular alternating lenses and interlayers of varied size and thickness that lie among the gabbroids of the upper mafic zone [13]. The lower part of the section is of interest due to the noble PGE mineralization associated mainly with orthopyroxenites, plagioclase-orthopyroxenites, and norites. The Western Nittis and Loypishnun deposits were discovered as a result of geological prospecting. According to Chashchin [13], they belong to a low-sulfide basal type of structure. The deposits are confined to the sulfide mineralization with a mean Pt + Pd content of up to 2 ppm; the ores have a Pd/Pt ratio of 1.7 and low contents of Ni and Cu.

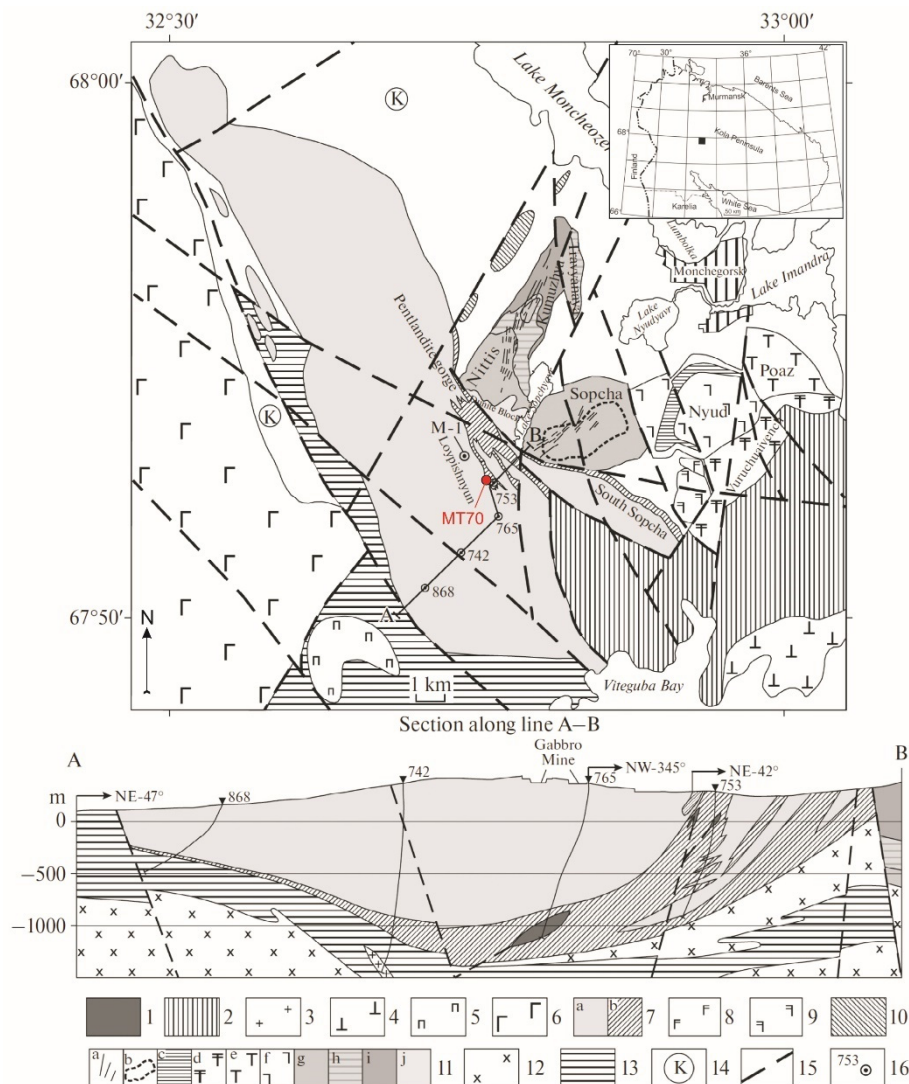


**Figure 1.** Scheme of the geological structure of the Monchetundra massif and Monchepluton with a section along the A–B line after [13]. (1) Metadunite and metaharzburgite; (2) Paleoproterozoic Imandra-Varzuga rift structure: metabasalt, metaandesibasalt, metarhyolite, and metadacite, quartzite and a schist of varied composition; (3) microcline–plagioclase granite; (4) layered mafic intrusions of the Imandra complex; (5) Ostrovsky layered massif, from peridotite to gabbro-norite; (6) Chunutundra intrusion complex of the Main Ridge: anorthosite, leucogabbro, gabbro-norite, and leuconorite; (7) Monchetundra massif: leucogabbro and gabbro-norite of upper zone (a), norite and orthopyroxenite of lower zone (b); (8) quartz metagabbro of massif 10 anomaly; (9) norite and metanorite of Lake Moroshkovoe massif; (10) gabbro-norite and metanorite of Kirikha massif; (11) Monchepluton: Cu–Ni ore vein (a), Sopcha ore bed 330 (b), olivine norite and orthopyroxenite (c), metagabbro of Vurechuaivench foothill massif (d), gabbro-norite (e), norite (f), orthopyroxenite (g), interbedding of orthopyroxenite and harzburgite (h), harzburgite (i), dunite (j); (12) diorite gneiss and quartz diorite gneiss; (13) Neoproterozoic Tersky–Allarechensky greenstone belt: amphibolite, biotite-amphibolite, and biotite plagioclase; (14) Paleo-Neoproterozoic metamorphic and ultrametamorphic units of Kola Block; (15) faults; (16) structural boreholes and their numbers.

### 3. Materials and Methods

Geochemical features of rocks in the lower zone of the massif were studied using drill core samples from the borehole MT-70 in the south-eastern slope of the Monchetundra massif. According to the data of the CJSC Terskaya Mining Company (Monchegorsk), the borehole intersects the ore zone 1 of the Loypishnun deposit (Figure 1).

Concentrations of petrogenic elements were estimated by atomic absorption spectrometer AAnalyst 400 (PerkinElmer Inc., Waltham, MA, USA) (wt.%) in the Laboratory for Chemical Analysis No. 33 of GI KSC RAS, Head of Laboratory L.I. Konstantinova. Analytical errors were 0.02–0.05%. The content of REE and disseminated elements was estimated by the ICP-MS method (ELEMENT, Thermo Fisher Scientific Inc., Waltham, MA, USA) for multi-element and isotope research in the Analytical Centre of V.S. Sobolev Institute of Geology and Mineralogy (IGM SB RAS, Novosibirsk, Russia), analyst I.V. Nikolaeva. The precision of the ICP-MS measurements was better than  $\pm 3\%$  for most elements. The PGE content in the massif rocks was measured by ICP-MS at ELAN-6100 DRC-e (PerkinElmer Inc., Waltham, MA, USA) in the Central Laboratory of A.P. Karpinsky Russian Geological Research Institute (VSEGEI, St. Petersburg, Russia), analysts V.A. Shilov and V.L. Kudryashov. The precision of the ICP-MS measurements was  $\pm 5\%$ .

The isotope Nd and Sr content was estimated with a Finnigan-MAT 262 (RPQ) (Thermo Fisher Scientific Inc., Waltham, MA, USA) solid-phase multicollector mass-spectrometer and a MI-1201 (NPO “Electron”, Sumy, Ukraine) mass-spectrometer in the Kola Centre for Geochronological and Isotope-Geochemical Research of GI KSC RAS (Apatity).

### 3.1. Sm-Nd Method

The samples for Sm-Nd analysis were treated using the ordinary techniques: dissolution in HF + HNO<sub>3</sub> (or + HClO<sub>4</sub>) in Teflon beakers at 100 °C following the extraction of Sm and Nd by ion-exchange column chromatography. Nd and Sm were measured by the isotopic dilution technique with a mixed <sup>149</sup>Sm/<sup>150</sup>Nd tracer on double Re + Re filaments. The measured reproducibility for the seven-parallel analysis of Nd-isotope composition for the standard JNdi-1 [14] was  $0.512089 \pm 14$ . The blanks for laboratory contamination for Nd and Sm were 0.3 and 0.06 ng, respectively. The reproducibility of measurements was  $\pm 0.3\%$  ( $2\sigma$ ) for <sup>147</sup>Sm/<sup>144</sup>Nd ratios in BCR-2 standard ( $N = 7$ ; [15]). The reproducibility of measurements for Nd-isotope composition was up to 0.01% ( $2s$ ) in an individual analysis. All <sup>147</sup>Sm/<sup>144</sup>Nd and <sup>143</sup>Nd/<sup>144</sup>Nd ratios were normalized to <sup>146</sup>Nd/<sup>144</sup>Nd = 0.7219 and adjusted to <sup>143</sup>Nd/<sup>144</sup>Nd = 0.512115 using the JNdi-1 standard [14]. The  $\epsilon_{\text{Nd}}(T)$  values were calculated using the following parameters of CHUR [16]: <sup>143</sup>Nd/<sup>144</sup>Nd = 0.512630 and <sup>147</sup>Sm/<sup>144</sup>Nd = 0.1960 and DM [17]: <sup>143</sup>Nd/<sup>144</sup>Nd = 0.513151 and <sup>147</sup>Sm/<sup>144</sup>Nd = 0.2136.

### 3.2. Rb-Sr Method

The Sr isotope compositions and Rb and Sr content were from a MI-1201 mass spectrometer by the isotopic dilution technique with the derived <sup>85</sup>Rb and <sup>84</sup>Sr tracers in a two-band mode using Re filaments. The isotope Sr composition in all measured samples was normalized to a value of 0.710235 as recommended by NBS SRM-987. The errors in the Sr isotope analysis (confidence interval of 95%) were up to 0.04%, and those of the Rb-Sr ratio determination were 1.5%. The blank laboratory contamination was 2.5 ng for Rb and 1.2 ng for Sr. The adopted Rb decay constant of [18] was used for the ISr calculations.

## 4. Results

### 4.1. Petrography

The top part of the section is represented by medium-grained amphibolized gabbro-norites (Figure 2) of the upper zone trachytoid gabbro-norites (2.5 Ga). These rocks host poorly preserved primary magmatic minerals; pyroxenes are highly amphibolized, secondary minerals are formed on plagioclase (groups of epidote, apatite, etc.), almost completely replacing the grains. This rock group contains bodies of coarse-grained, rarely pegmatoid melanocratic amphibolized gabbroids that seem to be related to massive gabbro-norites (2.47 Ga) or gabbro-pegmatites (2.45 Ga). The lower zone is represented by intercalated rocks of the norite and pyroxenite groups. The norite group comprises melano-, meso-, rarely leucocratic norites, including olivine-bearing varieties. The



pyroxenite group is represented by orthopyroxenites and Pl-orthopyroxenites, mainly. Both groups contain amphibolized rock varieties. According to Chashchin [19], the rocks were altered by the intense impact of fluids at the late and post-magmatic stages of the ore formation. The sulfide mineralization with a pentlandite-chalcopyrite-pyrrhotite composition dominates in rocks of this layered series and associates with the PGE mineralization [13].

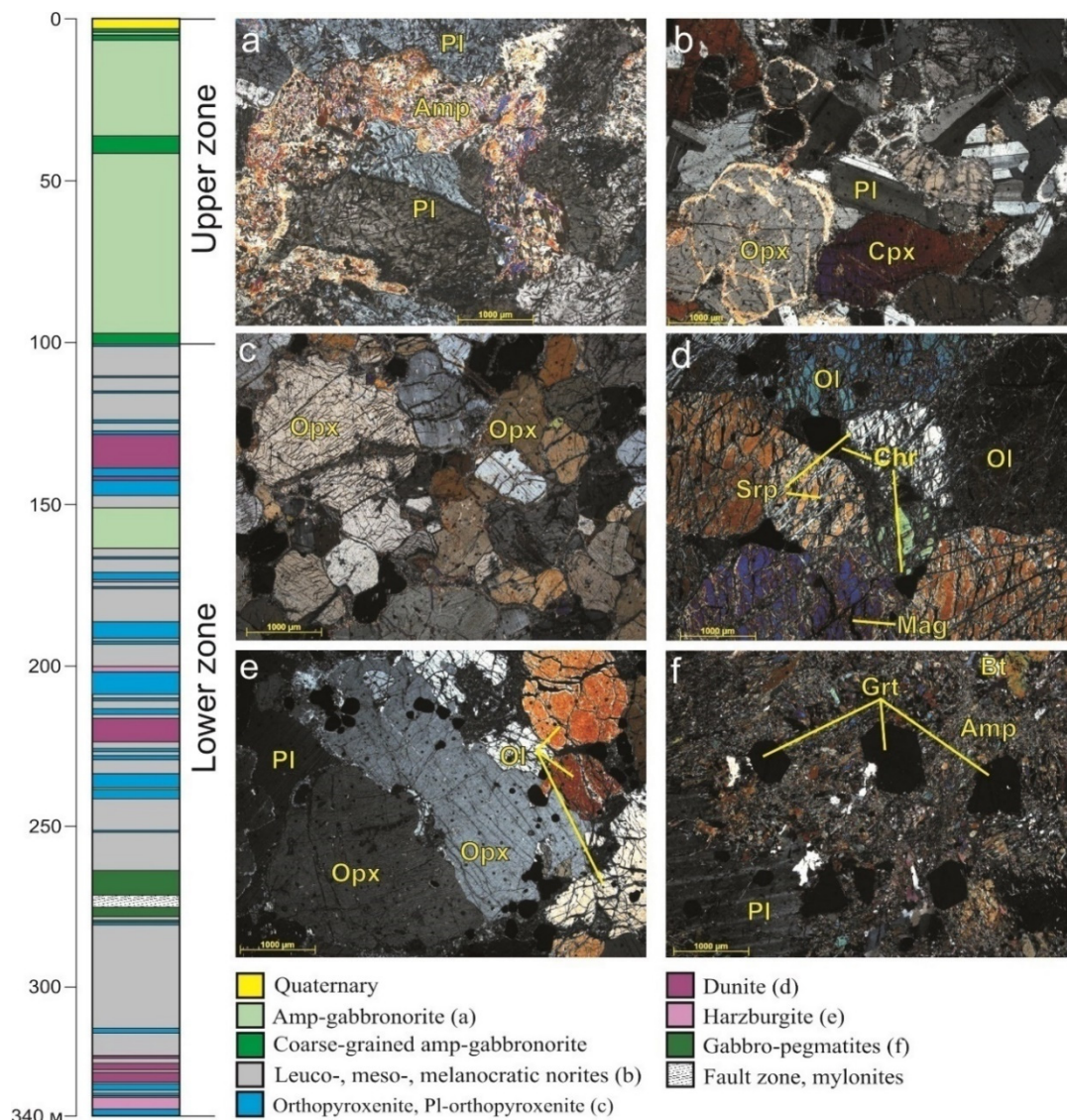


**Figure 2.** Schematic section of borehole MT-70 modified after [20] and pictures of thin sections of typical rocks from the Loypishnun area. Pl—plagioclase; Amp—amphibole; Opx—orthopyroxene; Cpx—clinopyroxene; Ol—olivine; Srp—serpentine; Chr—chromite; Mag—magnetite; Grt—garnet; Bt—biotite.

Bodies of dunites and harzburgites occur as 10-m thick interlayers in a stratified series of the lower zone. Dunites show well-preserved olivine grains with serpentine-magnetite and carbonate veinlets in them (Figure 2). Chromite grains are present in the amount of 1–3%. Harzburgites consist of olivine (50%), orthopyroxene (40%), plagioclase (5%), and clinopyroxene (2%). Additionally, there are rounded chromite grains associated with orthopyroxenes and olivines (Figure 2).

The interval of ~270 m is marked with a tectonic zone, where rocks are transformed into mylonites (Figure 2). Coarse-grained amphibolized gabbro-norites are widespread under and over this zone. Primary mafic minerals are almost completely replaced by amphibole; isometric grains of garnet

are abundant (up to 10%) here (Figure 2). Garnet occurs both as individual grains up to 3 mm in size and as their 3-cm long clusters. The rocks differ from amphibolized gabbro-norites of the upper borehole section in their mineralogical composition (plagioclase, garnet, amphibole, and biotite), structural, and textural features. These rocks are more like gabbro-pegmatites from the upper parts of the Monchetundra massif section (2.45 Ga).

#### 4.2. PGE Content

The PGE content was determined in order to reveal the relation between geochemical features and the PGE content in rocks (Table 1). Three areas with an elevated total PGE content were detected within the studied borehole section. They were confined to rocks in the lower zone, i.e., the intervals 177–194 m, 225–259 m, and 318–320 m. These areas host intercalated pyroxenites and norites; the rocks are often metamorphically altered, and primary pyroxenes are replaced by amphiboles. The elevated PGE content was directly related to an increase in the content of sulfide minerals in the rock. An elevated PGE content was also observed in the interval of 264–275 m, but in gabbro-pegmatites. Notably, all rocks in the borehole section exhibited the prevalence of Pd over Pt.

**Table 1.** The platinum group elements (PGE) content in Loypishnun area rocks, according to the MT-70 borehole section.

Sample	Petrography	Ru, ppm	Rh, ppm	Pd, ppm	Ir, ppm	Pt, ppm	Total	Pd/Pt
70/9	AGN	<1.d.	<1.d.	0.049	<1.d.	0.025	0.07	1.96
70/21	AGN	<1.d.	0.006	0.150	<1.d.	0.010	0.17	15.00
70/40	AGN	<1.d.	<1.d.	0.036	<1.d.	0.004	0.04	9.23
70/62	AGN	<1.d.	0.003	0.150	<1.d.	0.008	0.16	20.00
70/81	AGN	<1.d.	0.004	0.190	<1.d.	0.018	0.21	10.56
70/93	AGN	<1.d.	<1.d.	0.070	<1.d.	0.002	0.07	29.17
70/104	N	<1.d.	<1.d.	0.054	<1.d.	0.034	0.09	1.59
70/127	PX	<1.d.	<1.d.	0.039	<1.d.	0.018	0.06	2.17
70/127.6	N	<1.d.	<1.d.	0.031	<1.d.	0.014	0.05	2.21
70/129	DN	0.011	<1.d.	0.010	0.004	0.006	0.03	1.75
70/137	DN	0.013	<1.d.	0.004	0.004	0.003	0.02	1.39
70/151	N	<1.d.	0.005	0.190	0.002	0.100	0.30	1.90
70/157	AGN	<1.d.	0.002	0.130	<1.d.	0.004	0.14	35.14
70/165	PX	<1.d.	<1.d.	0.056	<1.d.	0.037	0.09	1.51
70/170	N	<1.d.	0.003	0.110	<1.d.	0.044	0.16	2.50
70/172	PX	<1.d.	0.003	0.053	<1.d.	0.024	0.08	2.21
70/177	N	0.005	0.042	1.350	0.008	0.400	1.80	3.38
70/189	PX	0.005	0.029	0.970	0.007	0.600	1.61	1.62
70/194	PX	0.003	0.021	0.590	0.005	0.170	0.79	3.47
70/196	N	<1.d.	0.004	0.160	<1.d.	0.033	0.20	4.85
70/200	HB	0.006	0.005	0.100	0.002	0.047	0.16	2.13
70/204	PX	0.012	0.005	0.086	0.005	0.055	0.16	1.56
70/214	N	<1.d.	0.006	0.180	<1.d.	0.048	0.23	3.75
70/219	DN	0.008	<1.d.	0.007	<1.d.	0.008	0.02	0.86
70/225	PX	0.003	0.016	0.570	0.004	0.300	0.89	1.90
70/245	N	0.005	0.028	0.800	0.007	0.470	1.31	1.70
70/259	N	0.003	0.025	0.790	0.005	0.430	1.25	1.84
70/264	GP	<1.d.	0.027	0.520	0.004	0.290	0.84	1.79
70/275	GP	0.003	0.048	0.390	0.003	0.170	0.61	2.29
70/281	N	<1.d.	0.660	0.160	0.008	0.079	0.91	2.03
70/303	N	<1.d.	<1.d.	0.094	<1.d.	0.015	0.11	6.27
70/319	N	0.003	0.005	0.370	0.002	0.230	0.61	1.61
70/324	DN	0.008	0.005	0.034	0.003	0.010	0.06	3.58

Detection limits (l.d.) for all elements are 0.002 ppm. AGN—Amp-gabbro-norites; N—norites; DN—dunites; PX—pyroxenites; HB—harzburgite; and GP—gabbro-pegmatites.

### 4.3. Whole Rocks Geochemistry

The  $\text{SiO}_2$  vs.  $(\text{Na}_2\text{O} + \text{K}_2\text{O})$  plot [21] (Table S1; Figure 3) shows that rocks from the MT-70 borehole section mainly occurred in the gabbroid field, and that amphibolized gabbro-norites had a higher total alkali content compared to norites, pyroxenites, and harzburgite. The composition of one gabbro-pegmatite sample is similar to that of diorites. Dunites are low in alkali and silica. Ore-bearing rocks have a slightly elevated alkali content compared to their barren analogues.

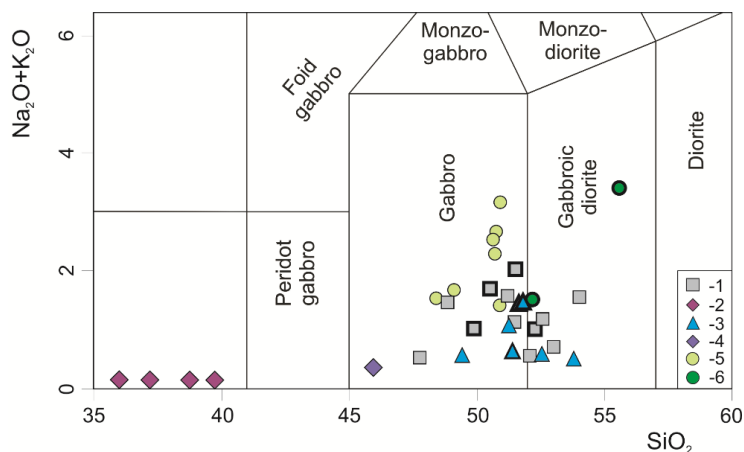


**Figure 3.**  $\text{SiO}_2$  vs.  $(\text{Na}_2\text{O} + \text{K}_2\text{O})$  plot (wt.%) after [21] for Loypishnun area rocks. 1—norites; 2—dunites; 3—pyroxenites; 4—harzburgite; 5—Amp-gabbro-norite; 6—gabbro-pegmatite. Ore-bearing rocks are marked in bold. Fields of rocks according to [21].

Variation plots on the MgO content (Figure 4) indicate that rocks from the MT70 borehole section produced quite regular increasing trends in  $\text{Al}_2\text{O}_3$ ,  $\text{Na}_2\text{O}$ , and  $\text{CaO}$  with a decrease in MgO. Notably, there were also increasing trends in the iron content (except for amphibolized gabbro-norites),  $\text{K}_2\text{O}$  and  $\text{TiO}_2$  with a decrease in MgO.

In general, the variation plots exhibited clear differentiation trends, i.e., dunites-harzburgites-orthopyroxenites-norites; these were less obvious for the gabbro-norites. Ore-bearing rocks have quite similar content of main oxides, except for  $\text{Al}_2\text{O}_3$  and  $\text{FeO}_t$ , which vary greatly (Table S1). Additionally, the alkali content is generally higher in ore varieties.

Multi-element distribution plots of primitive mantle-normalized REE and rare elements [22] show that the harzburgite, pyroxenites, and norites, including ore samples, have similar distribution spectra (Table S1; Figure 5). The spectra exhibited a weak negative slope, clear negative Nb anomaly, and weak positive Sr anomaly. However, the ore samples had a high mean content of large-ion lithophile elements (Ba, Rb, and Cs). We assumed that diverse compositions of norites in the lower zone, the mentioned features of ore norites and pyroxenites, were caused by the significant impact of fluids on the ore formation [19]. The spectra of amphibolized gabbro-norites are similar to those of gabbro-norites in the upper parts of the massif section [5]. They are characterized by negative Nb and positive Sr anomalies. Dunites are low in REE and disseminated elements compared to other rocks. Harzburgite occupies an intermediate position between the dunite and orthopyroxenites spectra. Ultramafic rocks, except for one sample of dunites, have a negative Nb anomaly as well. The form of spectra in gabbro-pegmatites is similar to that described for the section rocks, but as crystallization products of the residual melt, these rocks are irregularly enriched in almost all REE and rare elements (Figure 5).

The plots of chondrite-normalized REE distribution [23] (Table S2; Figure 5) in barren norites and pyroxenites show similar weakly differentiated spectra (the mean values of  $(\text{La}/\text{Yb})_n$  are 2.39 and 1.60, respectively) and an almost complete absence of Eu anomalies (the mean values of  $\text{Eu}/\text{Eu}^*$  are 0.95 and 0.87, respectively). However, there are more and less REE-rich samples of norites. The total REE content varies from 6.06 to 47.51 ppm; enriched varieties have a more differentiated spectrum

$(\text{La/Yb})_n = 3.31\text{--}5.56$ . Compared to barren varieties, ore norites and pyroxenites ( $\Sigma\text{PGE} > 0.5$  ppm) exhibit a more differentiated distribution spectrum with LREE prevalent over HREE; the mean values of  $(\text{La/Yb})_n$  are 3.64 and 2.88, respectively. Additionally, most samples of ore norites and ore pyroxenites show  $\text{Eu}/\text{Eu}^* \geq 1$  and a weak positive Eu anomaly.

Dunites are characterized by a low REE content of 0.67 to 1.97 ppm and a negative Eu anomaly  $\text{Eu}/\text{Eu}^*$  of 0.36–0.80. The spectrum slope fluctuates from weakly positive ( $(\text{La/Yb})_n = 0.81$ ) to negative in varieties rich in chromite mineralization ( $(\text{La/Yb})_n = 3.11$ ). Harzburgite exhibits an elevated total REE content compared to dunites (3.96 ppm), a weakly positive Eu anomaly ( $\text{Eu}/\text{Eu}^* = 1.20$ ), and a negative slope of the REE distribution spectrum ( $(\text{La/Yb})_n = 2.05$ ). Amphibolized gabbro-norites in the upper part of the borehole section show a moderate REE content (mean value—14.20 ppm), a positive Eu anomaly ( $\text{Eu}/\text{Eu}^* = 1.27\text{--}1.78$ ) and a slight prevalence of LREE over HREE (mean values  $(\text{La/Yb})_n = 1.78$ ). Amphibolized gabbro-norites significantly differ from gabbro-pegmatites, which have similar characteristics with later gabbro-pegmatites in the upper parts of the massif sections [6].

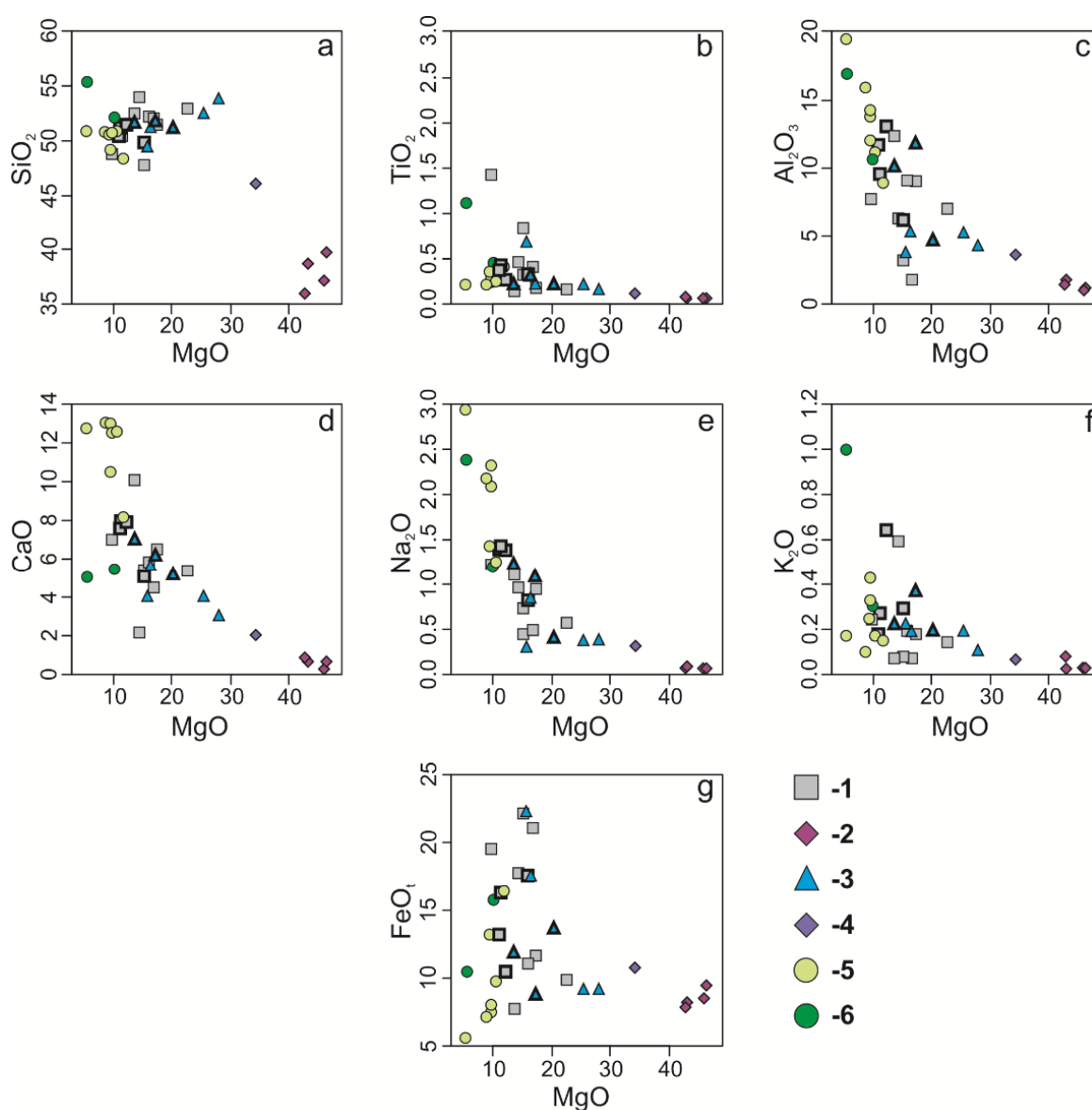


**Figure 4.** MgO vs. major oxides plot (a–g) (wt.%) for the Loypishnun area rocks. 1—norites; 2—dunites; 3—pyroxenites; 4—harzburgite; 5—mp-gabbro-norite; 6—gabbro-pegmatite; ore-bearing rocks are marked in bold.



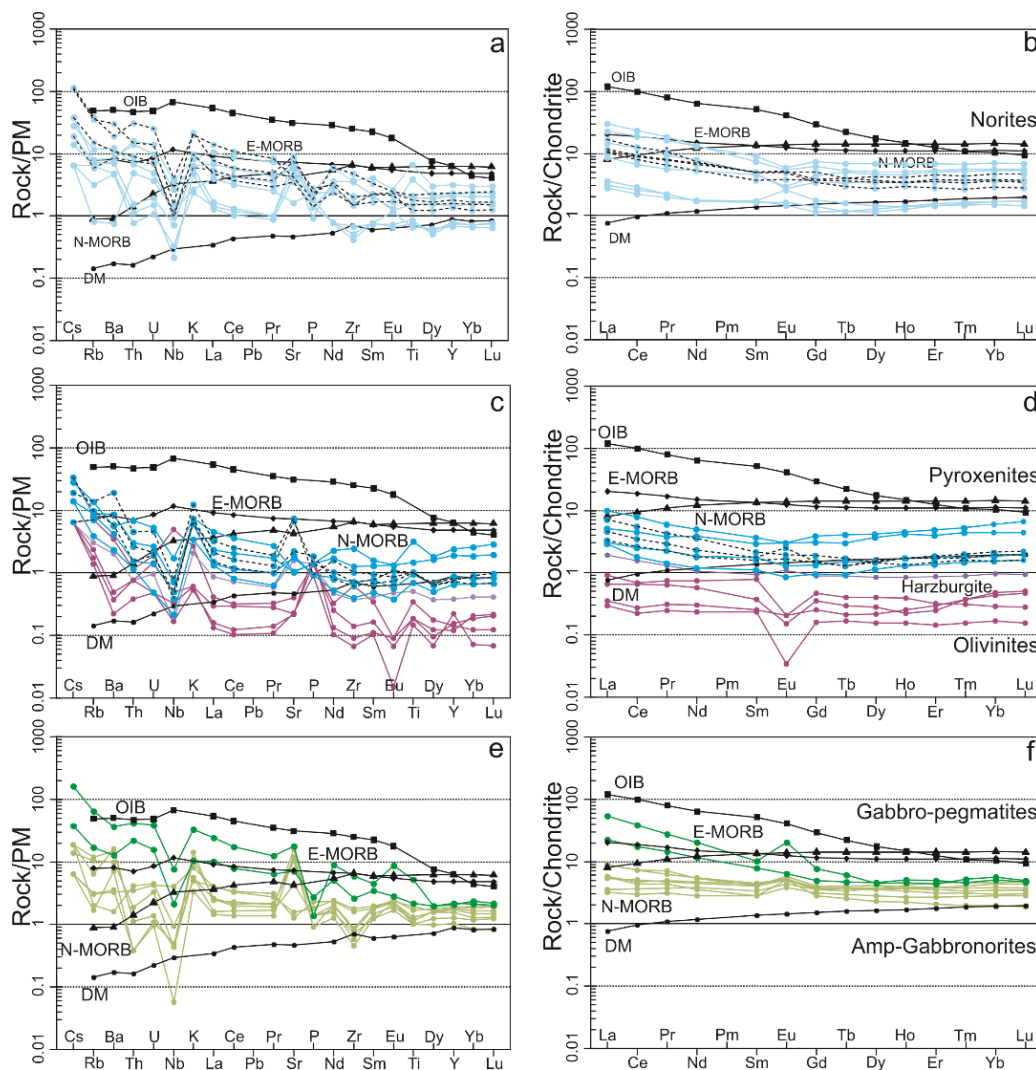


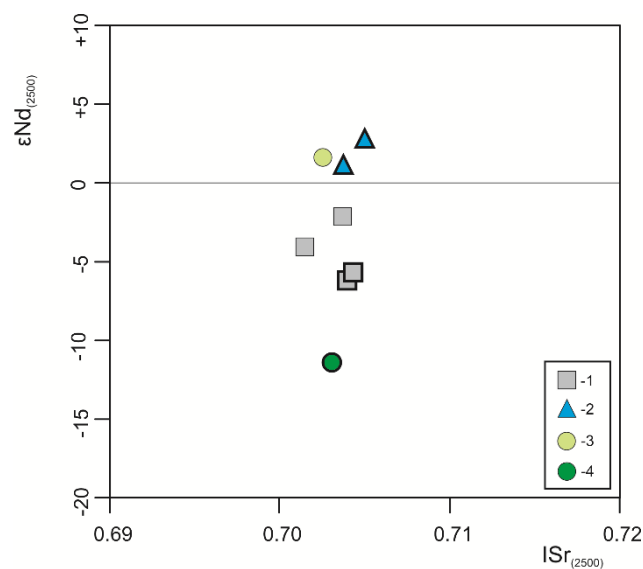
**Figure 5.** Primitive mantle (PM)-normalized [22] trace elements and chondrite-normalized [23] REE distribution plots (a–g) for the Loypishnun area rocks. Data on average normal mid-ocean ridge basalt (N-MORB), enriched mid-ocean ridge basalt (E-MORB), oceanic island basalt (OIB), and depleted mantle (DM) shown by black lines are after [22]. Dotted lines indicate the spectra of ore-bearing rocks (PGE > 0.5 ppm).

#### 4.4. Nd-Sr Isotope Composition

According to the isotope-geochemical Nd-Sr data (Table 2, Figure 6), dunites have weakly positive  $\epsilon\text{Nd}_{(2500)}$  values of +0.81 and low  $\text{ISr}_{(2500)}$  values of 0.69232 at the moment ca. 2.5 Ga. Clearly, such low values of  $\text{ISr}$  are hardly possible for dunites. Considering an intersecting mode of olivinite occurrence in the lower zone, they can be younger than 2.5 Ga. The  $\epsilon\text{Nd}_{(2500)}$  value in norites ranges from −4.13 to −2.16, while the  $\text{ISr}_{(2500)}$  value ranges from 0.70149 to 0.70433, respectively. Ore norites exhibit lower negative values of  $\epsilon\text{Nd}_{(2500)}$  (−5.72, −6.20) and  $\text{ISr}_{(2500)} = 0.704$ . Ore pyroxenites, on the contrary, have positive  $\epsilon\text{Nd}_{(2500)}$  values from +0.88 to +2.16 with similar  $\text{ISr}_{(2500)}$  values of about 0.704. The gabbro-pegmatites are characterized by low values of  $\epsilon\text{Nd}_{(2500)} = -11.65$  and  $\text{ISr}_{(2500)} = 0.7031$  ( $\text{ISr}_0 = 0.7191$ ). Amphibolized gabbro-norites in the upper parts of the borehole section exhibit  $\epsilon\text{Nd}_{(2500)} = +1.6$  and  $\text{ISr}_{(2500)} = 0.70253$ , while rocks breaking the lower zone rocks (interval 157 m) have higher  $\text{ISr}_{(2500)}$  values of 0.70494 (Table 2).

**Table 2.** The isotope Nd-Sr composition of Loypishnun area rocks.

Sample	Petrography	Rb, ppm	Sr, ppm	$^{87}\text{Rb}/^{86}\text{Sr}$	$^{87}\text{Sr}/^{86}\text{Sr}$	$\pm 2\sigma$ abs.	$I_{\text{Sr}(2500)}$	Sm, ppm	Nd, ppm	$^{147}\text{Sm}/^{144}\text{Nd}$	$^{143}\text{Nd}/^{144}\text{Nd}$	$\pm 2\sigma$ abs.	$\epsilon_{\text{Nd}(2500)}$
<b>70/21</b>	Amp-Gabbro-norite	1.08	251.91	0.0121	0.70297	0.00019	0.70253	0.48	1.66	0.1731	0.512334	0.000017	1.60
<b>70/104</b>	Norite	0.65	33.87	0.0541	0.70629	0.00022	0.70433	-	-	-	-	-	-
<b>70/151</b>	Norite	6.98	132.61	0.1486	0.70907	0.00016	0.70370	1.72	7.86	0.1319	0.511464	0.000004	-2.16
<b>70/157</b>	Amp-Gabbro-norite	9.29	264.00	0.0993	0.70853	0.00015	0.70494	-	-	-	-	-	-
<b>70/177</b>	Ore-Norite	24.72	187.74	0.3715	0.71769	0.00018	0.70426	0.81	3.58	0.1361	0.511351	0.000011	-5.72
<b>70/189</b>	Ore-Pyroxenite	5.45	49.22	0.3123	0.71627	0.00028	0.70498	0.27	1.10	0.1489	0.511987	0.000016	2.61
<b>70/214</b>	Norite	4.51	77.12	0.1650	0.70745	0.00014	0.70149	0.27	1.02	0.1616	0.511853	0.000019	-4.13
<b>70/225</b>	Ore-Pyroxenite	5.82	142.04	0.1157	0.70791	0.00016	0.70373	0.31	1.35	0.1378	0.511716	0.000029	0.88
<b>70/259</b>	Ore-Norite	9.09	156.30	0.1641	0.70990	0.00021	0.70397	0.99	3.65	0.1646	0.511797	0.000010	-6.20
<b>70/275</b>	Gabbro-pegmatite	63.94	407.30	0.4429	0.71908	0.00015	0.70340	1.90	9.06	0.1271	0.510901	0.000080	-11.64
<b>70/325</b>	Dunite	0.46	3.25	0.4056	0.70698	0.00022	-	0.06	0.22	0.1534	0.511970	0.000050	0.81

**Figure 6.** The initial isotope Nd-Sr composition for Loypishnun area rocks. 1—norites; 2—pyroxenites; 3—amp-gabbro-norite; 4—gabbro-pegmatite. Ore-host rocks are marked in bold.

## 5. Discussion

The obtained geochemical and isotope-geochemical data indicate that rocks in the lower zone of the Monchetundra massif have a moderate total REE content, which increases in the ore samples (Figure 7). Such pattern is observed in the  $(La/Yb)_n$  ratio, and the  $\epsilon Nd_{(2500)}$  in ore varieties decreases from positive to low negative values. Compared to other rocks, ore-bearing norites and pyroxenites show a weak positive Eu/Eu\* anomaly. Noteworthy, rocks at the interval of 100–170 m of the lower zone have a negative Eu/Eu\* anomaly, in contrast to the positive anomaly in superposed rocks of the upper zone. The initial  $Isr_{(2500)}$  ratios in ore-bearing rocks have similar values and tend to be similar with barren analogues, except for one analysis of norite and dunite.

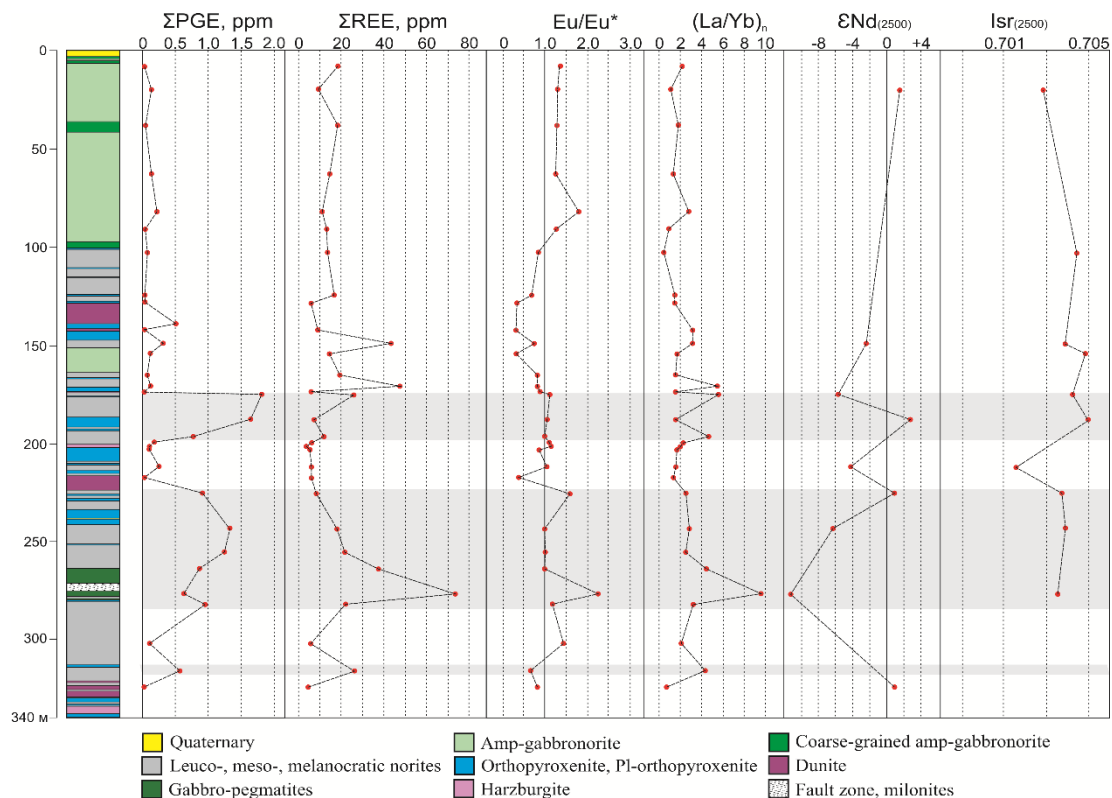


**Figure 7.** Summarized data on petrographic, PGE, REE, and Nd-Sr for MT-70 borehole rocks. Fields indicate ore-bearing rocks with a total PGE content of  $>0.5$  ppm.

As shown by the Nb/Yb vs. Th/Yb plot, the rocks of the lower zone layered series (harzburgite-norite-pyroxenites groups) are derivatives of the crust-mantle relation (Figure 8a). This position of points indicates contamination with matter, whose composition conforms to the lower and middle continental crust, and ore-bearing rocks that are highly contaminated. The same trend is observed in the La/Sm vs. Nb/Th plot (Figure 8b). Notably, rocks in the upper part of the section show a lower degree of contamination, while some points correspond to fields of mantle sources, like N-MORB and E-MORB. This may indicate, not only a lower degree of contamination with the crustal material, but also a heterogeneous inflow of the matter from sublithospheric reservoirs to the source.

According to data on isotope Nd composition, rocks in the Loypishnun deposit show widely varied  $\epsilon Nd$  values (Figure 9). The most probable reason for this is the crustal contamination of the initial mantle melt with products of the continental crust, i.e., rocks of the Central-Kola Block that are host rocks in the massif. Some rocks have low positive  $\epsilon Nd$  values, which can be explained by the contamination processes. However, as the plot shows (Figure 9), some rocks have far lower negative  $\epsilon Nd$  values than rocks in the Central-Kola Block [22–24]. It is possible that the isotope Sm-Nd system in these rocks was affected by other factors, such as fluidization during the ore formation or tectonic

activation. Interestingly, ore pyroxenites have positive  $\epsilon\text{Nd}$  values, while barren and ore norites have only negative  $\epsilon\text{Nd}$  values, though some of the rocks neighbor each other (Figure 9). Considering this fact, we may conclude that ore-bearing systems are characterized by an “instable” isotope Sm-Nd system. Amphibolized gabbro-norites show positive  $\epsilon\text{Nd}$  values, which is common for rocks in the upper part of the massif section [5,6,8]. Gabbro-pegmatites have very low negative  $\epsilon\text{Nd}$  values, which is quite uncommon for gabbro-pegmatites in the upper parts of the section [5,6].

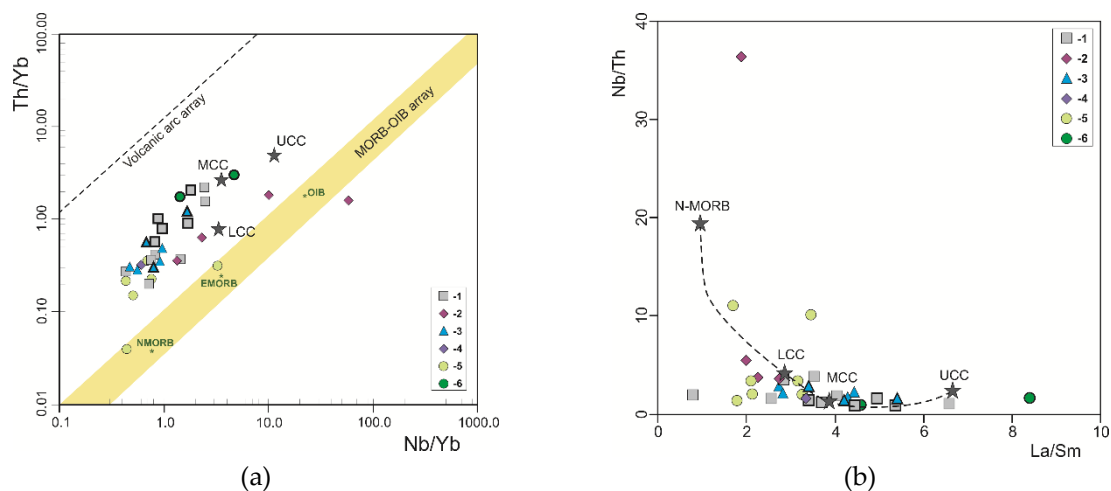


**Figure 8.** Plot Th/Yb vs. Nb/Yb (a) [24] and (b) La/Sm vs. Nb/Th (–) for MT-70 borehole rocks. 1—norites; 2—dunites; 3—pyroxenites; 4—harzburgite; 5—Amp-gabbro-norite; 6—gabbro-pegmatite. Continental crust composition according to [25]. Ore-bearing rocks are marked in bold.

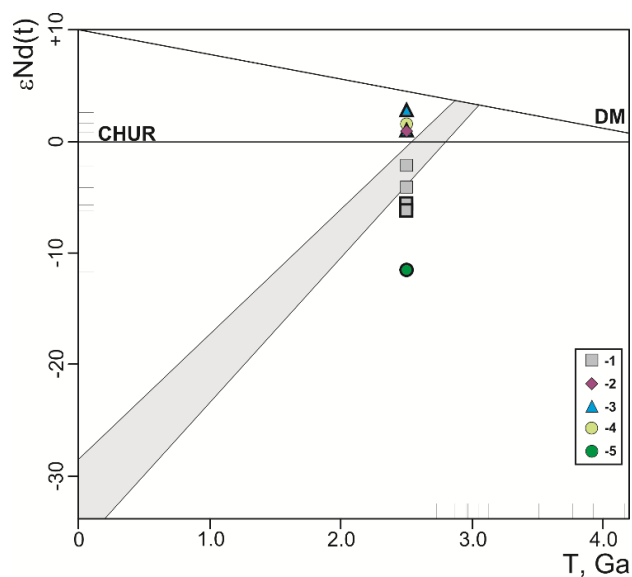


**Figure 9.**  $\epsilon\text{Nd}$ -T plot for Loypishnyn deposit rocks. 1—norites; 2—dunites; 3—pyroxenites; 4—amp-gabbro-norite; 5—gabbro-pegmatite; grey field—Central-Kola Block rocks [26–28]. Ore-bearing rocks are marked in bold.

According to [4,5,8,29–51], the intrusive magmatism at 2.53–2.39 Ga was widespread in the Fennoscandian Shield, Canada [52–55], and Zimbabwe [56]. The Paleoproterozoic massifs of the Fennoscandian Shield have similar initial isotope Nd-Sr values (Figure 10): the  $\epsilon\text{Nd}(i)$  values vary from  $-5$  to  $+3$ , the  $\text{ISr}(i)$  values range from 0.700 to 0.706, and their formation is related to the activity of the long-lived plume. In general, the isotope Nd-Sr compositions of rocks in the upper zone of the Monchetundra massif [4–6,8,29] are close to those in similar massifs, and the values of the



Amp-gabbronorite sample of the MT-70 borehole coincide as well. However, new studies of rocks in the lower zone indicate a wide range of values, first, on the isotope Nd composition. The ore norites show the greatest difference in values; however, as noted above, ore-bearing rocks have an “instable” isotope composition of Nd. The pattern of the gabbro-pegmatite isotope composition can be explained by transformation of the Sm-Nd system caused by the impact of fluids in the fault zone [34].

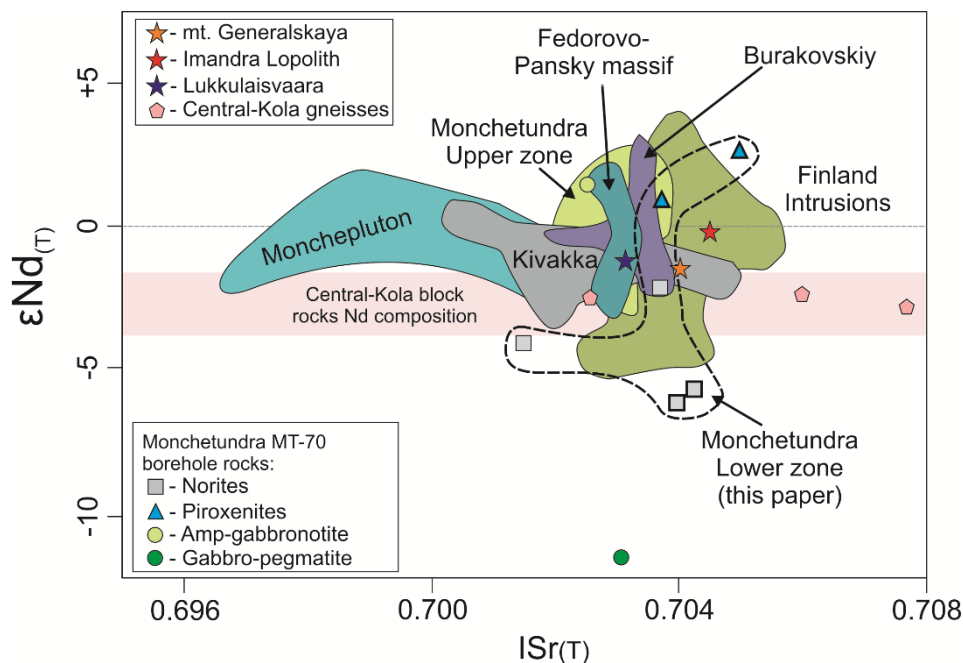


**Figure 10.** The  $\epsilon\text{Nd}$  vs.  $\text{ISr}$  plot for the Monchetundra rocks. Monchetundra massif upper zone, after [4,5,8,29]; Monchepluton massif rocks, after [4,29]; Fedorovo-Pansky massif after [29]; Mt. Generalskaya after [30]; Kivakka after [31,32], Burakovskiy, Lakkulaisvaara after [31]; Finland layered intrusions after [29,33] Field of Central-Kola Block rocks, after [26,27]; Central Kola gneisses, after [28]. Ore-bearing rocks are marked in bold.

According to [1,2,4], the evolution of Paleoproterozoic Monchepluton and Monchetundra massifs is confined to the long-lived mantle plume that preconditioned a high melting degree of rocks in the upper mantle [6]. As defined in [3], initial mantle melts were contaminated by the matter in the lower crust. New data on rocks from the lower zone of the Monchetundra massif show the contamination degree of their source to be higher than that of rocks from the upper part of the intrusion and the Monchepluton. New geochemical and isotope-geochemical data indicate that rocks from the layered intrusion of the Loypishnun deposit originated from a source with a generally low REE content, but a relatively LREE-rich. A clear Nb minimum, low Nb/Th ratios, high La/Sm, Nb/Yb, Th/Yb ratios, as well as relatively high  $\text{ISr}$  values and dominating low negative  $\epsilon\text{Nd}$  values indicate a considerable input of the crustal material to the source of initial magmas of these rocks.

The comparison of barren and ore-bearing varieties of norites and pyroxenites in the Loypishnun deposit shows that ore samples have the lowest negative  $\epsilon\text{Nd}$  values, a relatively more differentiated distribution spectrum with LREE dominating over HREE,  $\text{Eu}/\text{Eu}^* \geq 1$ , and higher mean contents of alkali and large-ion lithophile elements (Ba, Rb, and Cs).

The formation of ore bodies in the Loypishnun deposit with the basal type of structure [13] appears to be governed both by the crust-mantle interaction, magmatic differentiation, and association with the most differentiated varieties, and by further concentration of the ore at the late and post-magmatic stages in a highly permeable environment for fluids in the Monchetundra fault zone.

We also assumed that the initial melt of trachytoid gabbronorites in the upper zone (2.5 Ga) injected into already cooled rocks of the lower zone with no or a minimal amount of rocks from the

continental crust. Rocks in the upper part mainly interacted with those in the lower zone; therefore, they exhibit more “mantle” isotope characteristics.

**Supplementary Materials:** The following materials are available online at <http://www.mdpi.com/2075-163X/10/3/286/s1>, Table S1: Main oxides composition of Loypishnun area rocks, Table S2: Trace and rare earth elements of Loypishnun area rocks.

**Author Contributions:** Conceptualization, Visualization, Investigation and Writing—Original Draft Preparation E.K., E.B., L.N., P.S.; Investigation, P.S.; Methodology, P.S., D.E.; Supervision and Editing, T.B. All authors have read and agreed to the published version of the manuscript.

**Funding:** The study was funded by the Russian Foundation for Basic Research, grants No. 18-35-00152 mol\_a; 18-05-70082, research project No.0226-2019-0053.

**Acknowledgments:** The authors are grateful to L.I. Koval (GI KSC RAS) for sample preparation, L.I. Konstantinova, S.N. Dyakov, O.G. Sherstennikova, G.M. Sherstobitova (GI KSC RAS), I.V. Nikolaeva (IGM SBRAS), V.A. Shilov, V.L. Kudryashov (VSEGEI) for analytical works; M.S. Lyulko (CKE) for consultations and materials. The study was carried out with materials and the consent of CJSC Terskaya Mining Company (Monchegorsk).

**Conflicts of Interest:** The authors declare no conflict of interest.

## References

- Bayanova, T.; Ludden, J.; Mitrofanov, F. Timing and duration of Palaeoproterozoic events producing ore-bearing layered intrusions of the Baltic Shield: Metallogenic, petrological and geodynamic implications. *Geol. Soc. Lond. Spec. Publ.* **2010**, *323*, 165–198. [CrossRef]
- Mitrofanov, F.P.; Bayanova, T.B.; Korchagin, A.U.; Groshev, N.Y.; Malitch, K.N.; Zhirov, D.V.; Mitrofanov, A.F. East Scandinavian and Noril'sk plume mafic large igneous provinces of Pd-Pt ores: Geological and metallogenic comparison. *Geol. Ore Depos.* **2013**, *55*, 305–319. [CrossRef]
- Layered Intrusions of Monchegorsk Ore Region: Petrology, Ore-Forming, Isotopy, Deep Structure*; Mitrofanov, F.; Smolkin, V. (Eds.) KSC RAS: Apatity, Russia, 2004; p. 177.
- Yang, S.-H.; Hanski, E.; Li, C.; Maier, W.D.; Huhma, H.; Mokrushin, A.V.; Latypov, R.; Lahaye, Y.; O'Brien, H.; Qu, W.-J. Mantle source of the 2.44–2.50 Ga mantle plume-related magmatism in the Fennoscandian Shield: Evidence from Os, Nd, and Sr isotope compositions of the Monchepluton and Kemi intrusions. *Miner. Depos.* **2016**, *51*, 1055–1073. [CrossRef]
- Nerovich, L.I.; Bayanova, T.B.; Savchenko, Y.E.; Serov, P.A. Monchetundra massif: Geology, petrography, geochronology, geochemistry, PGE mineralization (new data). In *An Interreg-Tacis Project: Strategic Mineral Resources of Lapland – Base for the Sustainable Development of the North*; Project Publication; Mitrofanov, F., Iljina, M., Zhirov, D., Eds.; KSC RAS: Apatity, Russia, 2009; Volume II, pp. 97–112.
- Nerovich, L.I.; Bayanova, T.B.; Serov, P.A.; Elizarov, D.V. Magmatic sources of dikes and veins in the Moncha Tundra massif, Baltic Shield: Isotopic-geochronologic and geochemical evidence. *Geochem. Int.* **2014**, *52*, 605–624. [CrossRef]
- Borisenko, E.S.; Bayanova, T.B.; Nerovich, L.I.; Kunakkuzin, E.L. Paleoproterozoic mafic Monchetundra massif (Kola Peninsula): New geological and geochronological data. *Dokl. Earth Sci.* **2015**, *465*, 68–72. [CrossRef]
- Kunakkuzin, E.L.; Bayanova, T.B.; Nerovich, L.I.; Borisenko, E.S.; Serov, P.A.; Elizarov, D.V. New Nd-Sr isotope-geochemical research of the paleoproterozoic PGE-bearing Monchetundra massif rocks (Fennoscandian Shield). *Vestn. MSTU* **2015**, *18*, 269–279.
- Mitrofanov, F.P.; Pozhilenko, V.I.; Smolkin, V.F.; Arzamastsev, A.A.; Yevzerov, V.Y.; Lyubtsov, V.V.; Shipilov, E.V.; Nikolayeva, S.B.; Fedotov, Z.A. *Geology of Kola Peninsula*; Kola Science Centre RAS: Apatity, Russia, 1995; p. 145.
- Sharkov, E.V. *Formation of Layered Intrusions and Related Mineralization*; Nauchniy Mir: Moscow, Russia, 2006.
- Bayanova, T.B.; Nerovich, L.I.; Mitrofanov, F.P.; Zhavkov, V.A.; Serov, P.A. The Monchetundra basic massif of the Kola region: New geological and isotope geochronological data. *Dokl. Earth Sci.* **2010**, *431*, 288–293. [CrossRef]
- Mitrofanov, F.P.; Balagansky, V.V.; Balashov, Y.A.; Gannibal, L.F.; Dokuchaeva, V.S.; Nerovich, L.I.; Radchenko, M.K.; Ryungenen, G.I. U-Pb age of gabbro-anorthosite of the Kola Peninsula. *Dokl. Earth Sci.* **1993**, *331*, 95–98.

13. Chashchin, V.V.; Petrov, S.V.; Drogozhzhskaya, S.V. Loypishnyun low-sulfide Pt-Pd deposit of the Monchetundra basic massif, Kola Peninsula, Russia. *Geol. Ore Depos.* **2018**, *60*, 418–448. [\[CrossRef\]](#)
14. Tanaka, T.; Togashi, S.; Kamioka, H.; Amakawa, H.; Kagami, H.; Hamamoto, T.; Yuhara, M.; Orihashi, Y.; Yoneda, S.; Shimizu, H.; et al. JNdi-1: A neodymium isotopic reference in consistency with LaJolla neodymium. *Chem. Geol.* **2000**, *168*, 279–281. [\[CrossRef\]](#)
15. Raczek, I.; Jochum, K.P.; Hofmann, A.W. Neodymium and strontium isotope data for USGS reference materials BCR-1, BCR-2, BHVO-1, BHVO-2, AGV-1, AGV-2, GSP-1, GSP-2 and eight MPI-DING reference glasses. *Geostand. Geoanal. Res.* **2003**, *27*, 173–179. [\[CrossRef\]](#)
16. Bouvier, A.; Vervoort, J.D.; Patchett, P.J. The Lu–Hf and Sm–Nd isotopic composition of CHUR: Constraints from unequilibrated chondrites and implications for the bulk composition of terrestrial planets. *Earth Planet. Sci. Lett.* **2008**, *273*, 48–57. [\[CrossRef\]](#)
17. Goldstein, S.J.; Jacobsen, S.B. Nd and Sr isotopic systematics of river water suspended material implications for crystal evolution. *Earth Planet. Sci. Lett.* **1988**, *87*, 249–265. [\[CrossRef\]](#)
18. Steiger, R.; Jäger, E. Subcommission on geochronology: Convention on the use of decay constants in geo- and cosmochronology. *Earth Planet. Sci. Lett.* **1977**, *36*, 359–362. [\[CrossRef\]](#)
19. Chashchin, V.V.; Kul'chitskaya, A.A.; Elizarova, I.R. Fluid regime of the formation of low-sulfide PGM Loipishnyun deposits, Monchetundra mafic massif (Kola Peninsula, Russia). *Litosfera* **2017**, *17*, 91–109.
20. Lulko, M.S. Geological structure of Monchetundra massif Loypishnun area. *Tr. FNS* **2009**, 180–184.
21. Middlemost, E.A.K. Naming materials in the magma/igneous rock system. *Earth Sci. Rev.* **1994**, *37*, 215–244. [\[CrossRef\]](#)
22. Sun, S.; McDonough, W.F. Chemical and isotopic systematics of oceanic basalts: Implications for mantle composition and processes. *Geol. Soc. Lond. Spec. Publ.* **1989**, *42*, 313–345. [\[CrossRef\]](#)
23. Boynton, W.V. Cosmochemistry of the rare earth elements; meteorite studies. In *Rare Earth Element Geochemistry*; Henderson, P., Ed.; Elsevier Sci. Publ. Co.: Amsterdam, The Netherlands, 1984; pp. 63–114.
24. Pearce, J.A. Geochemical fingerprinting of oceanic basalts with applications to ophiolite classification and the search for Archean oceanic crust. *Lithos* **2008**, *100*, 14–48. [\[CrossRef\]](#)
25. Rudnick, R.L.; Fountain, D.M. Nature and composition of the continental crust—A lower crustal perspective. *Rev. Geophys.* **1995**, *33*, 267–309. [\[CrossRef\]](#)
26. Timmerman, M.J.; Daly, S.J. Sm–Nd evidence for late Archean crust formation in the Lapland-Kola Mobile Belt, Kola Peninsula, Russia and Norway. *Precambrian Res.* **1995**, *72*, 97–107. [\[CrossRef\]](#)
27. Petrovskaya, L.S.; Mitrofanov, F.P.; Bayanova, T.B.; Petrov, V.P.; Petrovsky, M.N. *Neoarchaean Enderbite-Granulite Complex of the Pulozero-Polnek-Tundra Region, Central-Kola Block: Stages and Thermodynamic Regime of Evolution (Kola Peninsula)*; Print. Kola Science Centre RAS: Apatity, Russia, 2010; p. 78.
28. Myskova, T.A.; Milkevich, R.I. The aluminous gneisses of Kola series, Baltic Shield (geochemistry, nature and age of protolith). *Tr. Kar. NC* **2016**, *10*, 34–62.
29. Bayanova, T.; Korchagin, A.; Mitrofanov, A.; Serov, P.; Ekimova, N.; Nitkina, E.; Kamensky, I.; Elizarov, D.; Huber, M. Long-lived mantle plume and polyphase evolution of palaeoproterozoic PGE intrusions in the Fennoscandian Shield. *Minerals* **2019**, *9*, 59. [\[CrossRef\]](#)
30. Balashov, Y.A.; Bayanova, T.B.; Mitrofanov, F.P. Isotope data on the age and genesis of layered basic-ultrabasic intrusions in the Kola Peninsula and Northern Karelia, Northeastern Baltic Shield. *Precambrian Res.* **1993**, *64*, 197–205. [\[CrossRef\]](#)
31. Amelin, Y.V.; Semenov, V.S. Nd and Sr isotopic geochemistry of mafic layered intrusions in the eastern Baltic shield: Implications for the evolution of Paleoproterozoic continental mafic magmas. *Contrib. Mineral. Petrol.* **1996**, *124*, 255–272. [\[CrossRef\]](#)
32. Revyako, N.M.; Kostitsyn, Y.A.; Bychkova, Y.V. Interaction between a mafic melt and host rocks during formation of the Kivakka layered intrusion, North Karelia. *Petrology* **2012**, *20*, 101–119. [\[CrossRef\]](#)
33. Mitrofanov, F.P.; Bayanova, T.B.; Ludden, J.N.; Korchagin, A.U.; Chashchin, V.V.; Nerovich, L.I.; Serov, P.A.; Mitrofanov, A.F.; Zhironov, D.V. Origin and exploration of the Kola PGE-bearing Province: New constraints from geochronology. In *Ore Deposits: Origin, Exploration, and Exploitation*; Sophie Decree, S., Robb, L., Eds.; Geophysical Monograph Series; Wiley: Hoboken, NJ, USA, 2019; pp. 3–36.
34. Sharkov, E.V.; Chistyakov, A.V.; Smol'kin, V.F.; Belyatskii, V.B.; Fedotov, Z.A. Age of the Moncha Tundra fault, Kola Peninsula: Evidence from the Sm–Nd and Rb–Sr isotopic systematic of metamorphic assemblages. *Geochem. Int.* **2006**, *44*, 317–326. [\[CrossRef\]](#)

35. Amelin, Y.V.; Heaman, L.M.; Semenov, V.S. U–Pb geochronology of layered mafic intrusions in the eastern Baltic Shield: Implications for the timing and duration of Paleoproterozoic continental rifting. *Precambrian Res.* **1995**, *75*, 31–46. [\[CrossRef\]](#)
36. Bayanova, T.; Mitrofanov, F.; Serov, P.; Nerovich, L.; Yekimova, N.; Nitkina, E.; Kamensky, I. Layered PGE Paleoproterozoic (LIP) intrusions in the N–E part of the Fennoscandian Shield—Isotope Nd–Sr and  $3\text{He}/4\text{He}$  data, summarizing U–Pb ages (on Baddeleyite and Zircon), Sm–Nd data (on Rock-Forming and Sulphide Minerals), duration and mineralization. In *Geochronology—Methods and Case Studies*; Morner, N.-A., Ed.; INTECH: London, UK, 2014; pp. 143–193.
37. Hanski, E.; Walker, R.J.; Huhma, H.; Suominen, I. The Os and Nd isotopic systematics of c. 2.44 Ga Akanvaara and Koitelainen mafic layered intrusions in northern Finland. *Precambrian Res.* **2001**, *109*, 73–102. [\[CrossRef\]](#)
38. Huhma, H.; Hanski, E.; Kontinen, A.; Vuollo, J.; Mänttäri, I.; Lahaye, Y. Sm–Nd and U–Pb isotope geochemistry of the Palaeoproterozoic mafic magmatism in eastern and northern Finland. *Geol. Surv. Finl. Bull.* **2018**, *405*, 150.
39. Huhma, H.; Clift, R.A.; Perttunen, V.; Sakko, M. Sm–Nd and Pb isotopic study of mafic rocks associated with early Proterozoic continental rifting: The Perapohja schist belt in northern Finland. *Contrib. Mineral. Petrol.* **1990**, *104*, 369–379. [\[CrossRef\]](#)
40. Krivolutskaya, N.A.; Svirskaya, N.M.; Belyatsky, B.V.; Smolkin, V.F.; Mamontov, V.P.; Fanygin, A.S. Geochemical Specifics of Massifs of the Drusite Complex in the Central Belomorian Mobile Belt: II. Sm–Nd Isotopic System of the Rocks and the U–Pb Isotopic System of Zircons. *Geochem. Int.* **2010**, *48*, 1064–1083. [\[CrossRef\]](#)
41. Maier, W.D.; Hanski, E.J. Layered mafic-ultramafic intrusions of Fennoscandia: Europe’s treasure chest of magmatic metal deposits. *Elements* **2017**, *13*, 415–420. [\[CrossRef\]](#)
42. Mitrofanov, F.; Golubev, A. Russian Fennoscandian metallogeny. In *Abstracts of the 33 IGC*; Norwegian Academy of Science and Letters: Oslo, Norway, 2008.
43. Schissel, D.; Tsvetkov, A.A.; Mitrofanov, F.P.; Korchagin, A.U. Basal platinum-group element mineralization in the fedorovpansky layered mafic intrusion, Kola Peninsula, Russia. *Econ. Geol.* **2002**, *97*, 1657–1677. [\[CrossRef\]](#)
44. Serov, P.A. Frontiers of Age Forming PGE Mineralization Fedorovo-Pansky Layered Intrusions in Sm–Nd and Rb–Sr Isotopic Characteristics. Ph.D. Thesis, Voronezh State University, Voronezh, Russia, 2008.
45. Serov, P. *Comparison between Sm–Nd Rock-Forming Mineral and U–Pb Zircon and Baddeleyite Data of the Fedorovo-Pansky Pt-bearing Layered Intrusion*; European Geosciences Union: Vienna, Austria, 2007; EGU2007-A-01156.
46. Serov, P. New Sm–Nd isotope-geochemical data for the Fedorovo-Pansky PGE-bearing layered intrusion (N–E Fennoscandian Shield). In *Geophysical Research Abstracts*; European Geosciences Union: Vienna, Austria, 2012; EGU2010–8143.
47. Serov, P.; Bayanova, T. Palaeoproterozoic Fedorovo-Pansky PGE-bearing layered intrusion of the N–E Baltic Shield: New isotope data. In *33 IGC*; Norwegian Academy of Science and Letters: Oslo, Norway, 2008.
48. Serov, P.; Ekimova, N.; Bayanova, T. Isotope-geochemical Nd–Sr evidence of Palaeoproterozoic plume magmatism in Fennoscandia and mantle-crust interaction on stages of layered intrusions formation. In *Geophysical Research Abstracts*; European Geosciences Union: Vienna, Austria, 2012; Volume 14, EGU2012–9113.
49. Serov, P.A.; Ekimova, N.A.; Bayanova, T.B.; Mitrofanov, F.P. Sulfide minerals as new geochronometers during Sm–Nd dating of the ore genesis for layered mafic and ultramafic intrusions. *Lithosphere* **2014**, *4*, 11–21.
50. Vogel, D.C.; Vuollo, J.I.; Alapieti, T.T.; James, R.S. Tectonic, stratigraphic and geochemical comparison between ca. 2500–2440 Ma mafic igneous events in the Canadian and Fennoscandian Shields. *Precambrian Res.* **1998**, *92*, 89–116. [\[CrossRef\]](#)
51. Ernst, R.E. *Large Igneous Provinces*; Cambridge University Press: Cambridge, UK, 2014; p. 653.
52. Heaman, L.M. 2.5–2.4 Ga global magmatism: Remnants or supercontinents or products of superplumes. *Geol. Soc. Am.* **2004**, *36*, 255.
53. James, R.S.; Easton, R.M.; Peck, D.C.; Hrominchuk, J.L. The East Bull Lake intrusive suite: Remnants of a 2.48 Ga large igneous and metallogenic province in the Sudbury area of the Canadian Shield. *Econ. Geol.* **2002**, *97*, 1577–1606. [\[CrossRef\]](#)



54. Ciborowski, T.J.R.; Kerr, A.C.; Ernst, R.E.; McDonald, I.; Minifie, M.J.; Harlan, S.S.; Millar, I.L. The early proterozoic Matachewan large Igneous Province: Geochemistry, petrogenesis, and implications for earth evolution. *J. Petrol.* **2015**, *56*, 1459–1494. [[CrossRef](#)]
55. Iljina, M.J.; Lee, C.A. PGE deposits in the marginal series of layered intrusions. In *Exploration for Platinum-Group Elements Deposits*; Mineralogical Association of Canada: Québec City, QC, Canada, 2005; pp. 75–96.
56. Söderlund, U.; Hofmann, A.; Klausen, M.B.; Olsson, J.R.; Ernst, R.E.; Persson, P.-O. Towards a complete magmatic barcode for the Zimbabwe craton: Baddeleyite U–Pb dating of regional dolerite dyke swarms and sill complexes. *Precambrian Res.* **2010**, *183*, 388–398. [[CrossRef](#)]



© 2020 by the authors. Licensee MDPI, Basel, Switzerland. This article is an open access article distributed under the terms and conditions of the Creative Commons Attribution (CC BY) license (<http://creativecommons.org/licenses/by/4.0/>).